Mechanics Research Communications 56 (2014) 123–129

Contents lists available at ScienceDirect

Mechanics Research Communications

journal homepage: www.elsevier.com/locate/mechrescom

On the effect of constraint parameters on the generalized displacement control method

Sofie E. Leon [a], Eduardo N. Lages [b], Catarina N. de Araújo [b], Glaucio H. Paulino [a,*]

[a] Department of Civil Engineering, University of Illinois, Urbana, IL, USA
[b] Center for Technology, Federal University of Alagoas, Maceió, Alagoas, Brazil

ARTICLE INFO

Article history:
Received 2 March 2013
Received in revised form 6 October 2013
Accepted 24 December 2013
Available online 7 January 2014

Keywords:
Nonlinear solution schemes
Generalized displacement control method
Arc-length control methods
Planar truss
Space truss

ABSTRACT

In this work, we investigate the generalized displacement control method (GDCM) and provide a modification (MGDCM) that results in an equivalent constraint equation as that of the linearized cylindrical arc-length control method (LCALCM). Through numerical examples, we illustrate that the MGDCM is more robust than the standard GDCM in capturing equilibrium paths in regions of high curvature. Moreover, we also provide a geometric and physical interpretation of the method, which sheds light on the general class of path following methods in structural mechanics.

1. Introduction

Arc-length control type algorithms are among the most popular and widely used for solving nonlinear problems because they consider simultaneous iteration on both load and displacement variables. The arc-length control method (ALCM) has had measured success in its various forms, which include spherical, cylindrical, elliptical, and linearized versions (Wempner, 1971; Riks, 1972, 1979; Ramm, 1980; Crisfield, 1981, 1983). However, in some cases difficulties in recovering equilibrium paths with various versions of the ALCM have been reported (Carrera, 1994; Feng et al., 1996; Ritto-Correa and Camotim, 2008).

To overcome issues of numerical stability near limit points associated with the ALCM, Yang and Shieh (1990) proposed the generalized displacement control method (GDCM). Since its introduction, the GDCM has been widely used for structural mechanics applications, including geometric nonlinear analysis of steel, concrete and composite frames, and thin structures. Additionally, it has been used in the development of several new beam, plate, and shell elements, which are suited for large deformations. Rather than using the GDCM to solve a complex nonlinear problem, this work is focused on analysis of the nonlinear solution method itself.

The success of the method in solving a nonlinear problem depends on the selection of an initial load factor. Typically, a small value is chosen to capture complex nonlinearities, but the method can yield poor or non-convergent results for slightly larger values of the load factor. In this work, we present a modification to the GDCM constraint equation that yields convergent results even at high values of the initial load factor. We will also show that this slight modification results in an equivalent formulation, namely in the constraint equation, as the linearized cylindrical arc-length control algorithm (LCALCM). Recently, the difference was briefly mentioned by Leon et al. (2011) but was not fully studied, hence, this paper investigates and elaborates on the methods in detail. In a related study, Cardoso and Fonseca (2007) also analyzed the GDCM and identified that it could be expressed as an orthogonal ALCM.

The remainder of this paper is organized as follows: Section 2 outlines the incremental-iterative procedure and introduces the nomenclature used in this work. Next the GDCM is presented in Section 3. In Section 4, we discuss the motivation for the modification to the GDCM and show that the resulting constraint equation is equivalent to that of the LCALCM. We highlight the difference between the original GDCM and the MGDCM through numerical examples in Section 5. Finally, concluding remarks are made in Section 6.

2. Incremental-iterative procedure

The discrete equilibrium equation is $\mathbf{f}(\mathbf{u}) = \lambda \mathbf{p}$, where the internal forces, $\mathbf{f}$, are a function of the displacements, $\mathbf{u}$, and the applied

* Corresponding author at: 205 N. Matthews Avenue, 3129 Newmark Lab, Urbana, IL 61801, USA. Tel.: +1 217 333 3817; fax: +1 217 265 8041.
E-mail addresses: leon7@illinois.edu (S.E. Leon), enl@lccv.ufal.br (E.N. Lages), catarina@lccv.ufal.br (C.N. de Araújo), paulino@illinois.edu, paulino@uiuc.edu (G.H. Paulino).

0093-6413/$ – see front matter © 2014 Elsevier Ltd. All rights reserved.
http://dx.doi.org/10.1016/j.mechrescom.2013.12.009

forces are given by the product of a reference load vector, $\mathbf{p}$, and the load factor, λ. If the external and internal forces are not in equilibrium in any deformed configuration, then a residual vector remains, i.e.

$$\mathbf{r} = \lambda\mathbf{p} - \mathbf{f}(\mathbf{u}) \tag{1}$$

Due to the nonlinear nature of this problem, an incremental-iterative procedure is typically adopted. At each incremental step, a series of iterations is performed until convergence is achieved. The incremental-iterative procedure is given by

$$\mathbf{K}^i_{j-1}(\mathbf{u}^i_{j-1})\Delta\mathbf{u}^i_j = \Delta\lambda^i_j\mathbf{p} + \mathbf{r}^i_{j-1}(\lambda^i_{j-1},\ \mathbf{u}^i_{j-1}) \tag{2}$$

where $\mathbf{K}$ is the tangent stiffness matrix. We denote the increment with the superscript i, and the iteration with the subscript j. The displacements and load factor are computed through additive contributions from each iteration, i.e.

$$\mathbf{u}^i_j = \mathbf{u}^i_{j-1} + \Delta\mathbf{u}^i_j \tag{3}$$

$$\lambda^i_j = \lambda^i_{j-1} + \Delta\lambda^i_j \tag{4}$$

In the jth iteration of the ith increment, the load factor is incremented by $\Delta\lambda^i_j$, and the resulting displacement, $\Delta\mathbf{u}^i_j$, is found. Then the total displacement and total load factor are updated according to Eqs. (3) and (4), respectively. The residual in Eq. (2) is given by

$$\mathbf{r}^i_{j-1}(\lambda^i_{j-1},\ \mathbf{u}^i_{j-1}) = \lambda^i_{j-1}\mathbf{p} - \mathbf{f}(\mathbf{u}^i_{j-1}) \tag{5}$$

The load factor is computed through the following constraint equation (Yang and Shieh, 1990)

$$\mathbf{a}^i_j \cdot \Delta\mathbf{u}^i_j + b^i_j\Delta\lambda^i_j = c^i_j \tag{6}$$

The constraint equation is defined by the nonlinear solution scheme – see Leon et al. (2011) for a review of several nonlinear solution schemes unified by this constraint equation. In this work, we will focus on the constraint equation associated with the GDCM. The augmented system now has $(N+1)$ unknowns, where N is the number of degrees of freedom in $\mathbf{u}$, and the additional unknown is associated with the load factor. We employ the strategy of Batoz and Dhatt (1979) where the vector of unknowns is decomposed into two parts

$$\Delta\mathbf{u}^i_j = \Delta\lambda^i_j\Delta\mathbf{u}_{\mathrm{p}}{}^i_j + \Delta\mathbf{u}_{\mathrm{r}}{}^i_j \tag{7}$$

such that Eq. (2) becomes two inter-related equations

$$\mathbf{K}^i_{j-1}\Delta\mathbf{u}_{\mathrm{p}}{}^i_j = \mathbf{p} \tag{8}$$

$$\mathbf{K}^i_{j-1}\Delta\mathbf{u}_{\mathrm{r}}{}^i_j = \mathbf{r}^i_{j-1} \tag{9}$$

Then the new constraint expression is given by

$$\Delta\lambda^i_j = \frac{c^i_j - \mathbf{a}^i_j \cdot \Delta\mathbf{u}_{\mathrm{r}}{}^i_j}{\mathbf{a}^i_j \cdot \Delta\mathbf{u}_{\mathrm{p}}{}^i_j + b^i_j} \tag{10}$$

3. Standard generalized displacement control method

In the original formulation of the GDCM, Yang and Shieh (1990) specified $\mathbf{a}^i_j = \Delta\lambda^i_1\Delta\mathbf{u}_{\mathrm{p}}{}^{i-1}_1$ and $b^i_j = 0$ to achieve numerical stability of the constraint equation (Eq. (10)), but with no physical or geometrical justification. The update to the load factor is given by

$$\Delta\lambda^i_j = \frac{c^i_j - \Delta\lambda^i_1(\Delta\mathbf{u}_{\mathrm{p}}{}^{i-1}_1 \cdot \Delta\mathbf{u}_{\mathrm{r}}{}^i_j)}{\Delta\lambda^i_1(\Delta\mathbf{u}_{\mathrm{p}}{}^{i-1}_1 \cdot \Delta\mathbf{u}_{\mathrm{p}}{}^i_j)} \tag{11}$$

where c^i_j is the so-called generalized displacement. The load factor is formulated such that the generalized displacement is prescribed on the first iteration of an increment (i.e., $c^i_1 = c$), and is unchanged at subsequent iterations (i.e., $c^i_{j>1} = 0$). Then the load factor is

$$\Delta\lambda^i_j = \begin{cases} \dfrac{c}{\Delta\lambda^i_1\Delta\mathbf{u}_{\mathrm{p}}{}^{i-1}_1 \cdot \Delta\mathbf{u}_{\mathrm{p}}{}^i_1} & j = 1 \\ -\dfrac{\Delta\mathbf{u}_{\mathrm{p}}{}^{i-1}_1 \cdot \Delta\mathbf{u}_{\mathrm{r}}{}^i_j}{\Delta\mathbf{u}_{\mathrm{p}}{}^{i-1}_1 \cdot \Delta\mathbf{u}_{\mathrm{p}}{}^i_j} & j > 1 \end{cases} \tag{12}$$

Special treatment of Eq. (12) is required for the first increment (i.e., $i=1$) because $\Delta\mathbf{u}_{\mathrm{p}}{}^0_1$ does not exist. Hence Yang and Shieh (1990) considered $\Delta\mathbf{u}_{\mathrm{p}}{}^0_1 = \Delta\mathbf{u}_{\mathrm{p}}{}^1_1$, which leads to the following definition of c,

$$c = (\Delta\lambda^1_1)^2\Delta\mathbf{u}_{\mathrm{p}}{}^1_1 \cdot \Delta\mathbf{u}_{\mathrm{p}}{}^1_1 \tag{13}$$

where $\Delta\lambda^1_1 = \overline{\Delta\lambda}$ is the prescribed initial load factor. At the first iteration of an increment, the load factor is

$$\Delta\lambda^i_1 = \frac{\overline{\Delta\lambda}^2\Delta\mathbf{u}_{\mathrm{p}}{}^1_1 \cdot \Delta\mathbf{u}_{\mathrm{p}}{}^1_1}{\Delta\lambda^i_1\Delta\mathbf{u}_{\mathrm{p}}{}^{i-1}_1 \cdot \Delta\mathbf{u}_{\mathrm{p}}{}^i_1} = \pm\overline{\Delta\lambda}\left|\mathrm{GSP}\right|^{1/2} \tag{14}$$

where the Generalized Stiffness Parameter (GSP) is

$$\mathrm{GSP} = \frac{\Delta\mathbf{u}_{\mathrm{p}}{}^1_1 \cdot \Delta\mathbf{u}_{\mathrm{p}}{}^1_1}{\Delta\mathbf{u}_{\mathrm{p}}{}^{i-1}_1 \cdot \Delta\mathbf{u}_{\mathrm{p}}{}^i_1} \tag{15}$$

The load factor update for the GDCM is summarized as:

$$\Delta\lambda^i_j = \begin{cases} \overline{\Delta\lambda} & j = 1 \\ -\dfrac{\Delta\mathbf{u}_{\mathrm{p}}{}^1_1 \cdot \Delta\mathbf{u}_{\mathrm{r}}{}^1_j}{\Delta\mathbf{u}_{\mathrm{p}}{}^1_1 \cdot \Delta\mathbf{u}_{\mathrm{p}}{}^1_j} & j > 1 \end{cases} \quad i = 1$$

$$\Delta\lambda^i_j = \begin{cases} \pm\overline{\Delta\lambda}\left|\dfrac{\Delta\mathbf{u}_{\mathrm{p}}{}^1_1 \cdot \Delta\mathbf{u}_{\mathrm{p}}{}^1_1}{\Delta\mathbf{u}_{\mathrm{p}}{}^{i-1}_1 \cdot \Delta\mathbf{u}_{\mathrm{p}}{}^i_1}\right|^{1/2} & j = 1 \\ -\dfrac{\Delta\mathbf{u}_{\mathrm{p}}{}^{i-1}_1 \cdot \Delta\mathbf{u}_{\mathrm{r}}{}^i_j}{\Delta\mathbf{u}_{\mathrm{p}}{}^{i-1}_1 \cdot \Delta\mathbf{u}_{\mathrm{p}}{}^i_j} & j > 1 \end{cases} \quad i > 1 \tag{16}$$

The sign of the load factor in Eq. (14) (similarly in Eq. (16) when $i>1$ and $j=1$) is determined by the sign of denominator of the GSP, i.e. $\mathrm{sign}(\Delta\lambda^i_1) = \mathrm{sign}(\Delta\mathbf{u}_{\mathrm{p}}{}^{i-1}_1 \cdot \Delta\mathbf{u}_{\mathrm{p}}{}^i_1)$. The sign of $\Delta\mathbf{u}_{\mathrm{p}}{}^{i-1}_1 \cdot \Delta\mathbf{u}_{\mathrm{p}}{}^i_1$ will change only when the equilibrium configuration contains a load limit point, which implies that the sign of $\Delta\lambda^i_1$ corresponds to the sign of the stiffness of the system.

By prescribing a small initial load factor, the GDCM has been used successfully to solve highly nonlinear systems. However, to the best knowledge of the authors, the robustness of the load factor has not been studied in detail. Therefore, it is the aim of this work to investigate the behavior of the load factor in the most complex regions of equilibrium paths.

In areas of high gradients near load limit points, the GSP of the GDCM may not accurately reflect the stiffness of the structure. Notice that the GSP relies on information from the previous (i.e. $\Delta\mathbf{u}_{\mathrm{p}}{}^{i-1}_1$) and current increment (i.e. $\Delta\mathbf{u}_{\mathrm{p}}{}^i_1$). If the curvature is high, then the inner product between the displacement vector from the first iteration of the previous increment and the first iteration of the current increment will be small, which will increase the GSP. Unless the user–prescribed initial load factor $\left(\overline{\Delta\lambda}\right)$ is very small, then the load factor will be too large. The overestimation of the load factor will cause the method to either skip over part of the equilibrium path or completely diverge. In Section 5 we will examine a numerical example with an analytical solution to show that the GDCM load factor is overestimated near limit points for several values of the prescribed initial load factor.

4. Modification to the generalized displacement control method

To remedy the problem of overestimating the load factor, the so-called modified GDCM (MGDCM) redefines the constraint equation by setting

$$\mathbf{a}_j^i = \Delta\lambda_1^i \Delta\mathbf{u}_{\mathrm{p}1}^i \tag{17}$$

Just as in the original GDCM, c_j^i represents the generalized displacement on the first iteration and is unchanged on subsequent iterations, thus the load factor is

$$\Delta\lambda_j^i = \begin{cases} \dfrac{c}{\Delta\lambda_1^i \Delta\mathbf{u}_{\mathrm{p}1}^i \cdot \Delta\mathbf{u}_{\mathrm{p}1}^i} & j = 1 \\ -\dfrac{\Delta\mathbf{u}_{\mathrm{p}1}^1 \cdot \Delta\mathbf{u}_{\mathrm{r}j}^i}{\Delta\mathbf{u}_{\mathrm{p}1}^1 \cdot \Delta\mathbf{u}_{\mathrm{p}j}^i} & j > 1 \end{cases} \tag{18}$$

and c is simply

$$c = \left(\Delta\lambda_1^1\right)^2 \Delta\mathbf{u}_{\mathrm{p}1}^1 \cdot \Delta\mathbf{u}_{\mathrm{p}1}^1 \tag{19}$$

where $\Delta\lambda_1^1 = \overline{\Delta\lambda}$ as before. At the first iteration of an increment, the load factor is

$$\Delta\lambda_1^i = \frac{\overline{\Delta\lambda}^2 \Delta\mathbf{u}_{\mathrm{p}1}^1 \cdot \Delta\mathbf{u}_{\mathrm{p}1}^1}{\Delta\lambda_1^i \Delta\mathbf{u}_{\mathrm{p}1}^i \cdot \Delta\mathbf{u}_{\mathrm{p}1}^i} = \pm\overline{\Delta\lambda}\left|\mathrm{GSP}\right|^{1/2} \tag{20}$$

and the GSP has changed slightly to

$$\mathrm{GSP} = \frac{\Delta\mathbf{u}_{\mathrm{p}1}^1 \cdot \Delta\mathbf{u}_{\mathrm{p}1}^1}{\Delta\mathbf{u}_{\mathrm{p}1}^i \cdot \Delta\mathbf{u}_{\mathrm{p}1}^i} \tag{21}$$

The sign of the load factor is handled as it was for the GDCM, where the sign of the inner product $(\Delta\mathbf{u}_{\mathrm{p}1}^{i-1} \cdot \Delta\mathbf{u}_{\mathrm{p}1}^i)$ determines the sign of the update to the load factor. Notice that information from the previous increment is only used to indicate the sign of the load factor, but is not used to calculate its magnitude, as is done in the original GDCM formulation. The load factor is summarized as

$$\Delta\lambda_j^i = \begin{cases} \overline{\Delta\lambda} & j = 1 \\ -\dfrac{\Delta\mathbf{u}_{\mathrm{p}1}^1 \cdot \Delta\mathbf{u}_{\mathrm{r}j}^1}{\Delta\mathbf{u}_{\mathrm{p}1}^1 \cdot \Delta\mathbf{u}_{\mathrm{p}j}^1} & j > 1 \end{cases} \quad i = 1$$

$$\Delta\lambda_j^i = \begin{cases} \pm\overline{\Delta\lambda}\left|\dfrac{\Delta\mathbf{u}_{\mathrm{p}1}^1 \cdot \Delta\mathbf{u}_{\mathrm{p}1}^1}{\Delta\mathbf{u}_{\mathrm{p}1}^i \cdot \Delta\mathbf{u}_{\mathrm{p}1}^i}\right|^{1/2} & j = 1 \\ -\dfrac{\Delta\mathbf{u}_{\mathrm{p}1}^i \cdot \Delta\mathbf{u}_{\mathrm{r}j}^i}{\Delta\mathbf{u}_{\mathrm{p}1}^i \cdot \Delta\mathbf{u}_{\mathrm{p}j}^i} & j > 1 \end{cases} \quad i > 1 \tag{22}$$

Next we will show that the modification to the GDCM results in the same constraint equation as the LCALCM. Eq. (20) can be reorganized as follows

$$\left(\Delta\lambda_1^i\right)^2 \Delta\mathbf{u}_{\mathrm{p}1}^i \cdot \Delta\mathbf{u}_{\mathrm{p}1}^i = \overline{\Delta\lambda}^2 \Delta\mathbf{u}_{\mathrm{p}1}^1 \cdot \Delta\mathbf{u}_{\mathrm{p}1}^1 \tag{23}$$

or

$$\left(\Delta\lambda_1^i \Delta\mathbf{u}_{\mathrm{p}1}^i\right) \cdot \left(\Delta\lambda_1^i \Delta\mathbf{u}_{\mathrm{p}1}^i\right) = \left(\overline{\Delta\lambda}\Delta\mathbf{u}_{\mathrm{p}1}^1\right) \cdot \left(\overline{\Delta\lambda}\Delta\mathbf{u}_{\mathrm{p}1}^1\right) \tag{24}$$

On the first iteration the residual is zero, so according to Eq. (7), $\Delta\mathbf{u}_1^i = \Delta\lambda_1^i \Delta\mathbf{u}_{\mathrm{p}1}^i$, then

$$\Delta\mathbf{u}_1^i \cdot \Delta\mathbf{u}_1^i = \overline{\Delta\mathbf{u}}_1^1 \cdot \overline{\Delta\mathbf{u}}_1^1 = \left(\overline{\Delta s}_1^1\right)^2 \tag{25}$$

Notice that Eq. (25) is the constraint equation of the cylindrical ALCM – see Crisfield (1981). We imposed $\Delta\mathbf{u}_1^i \cdot \Delta\mathbf{u}_j^i = 0$ when $j > 1$ by definition of c_j^i. If we apply the same constraint to Eq. (25), then we arrive at the same equation as that of the linearized version of the cylindrical ALCM. The constraint equation is not sufficient to solve a nonlinear problem, as the sign of the load factor increment must still be determined. A number of approaches could be used to estimate the stiffness of the structure and therefore the sign of the load factor increments. In this work, we use the sign of the denominator of the GDCM GSP as the sign of the load factor increment, as proposed by Yang and Shieh (1990).

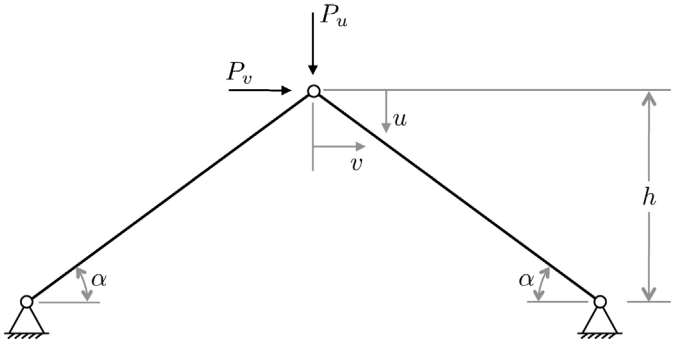

Fig. 1. Two-bar planar truss schematic.

5. Numerical examples

We explore the differences between the GDCM and MGDCM through two numerical examples. First we present a two bar truss subjected to two loading cases. A detailed explanation of the overestimation of the GDCM load factor increment is presented through this example. Next, a twelve bar truss is analyzed and the same inconsistency in the GDCM load factor is observed. To demonstrate that the behavior is not unique to a specially selected set of initial conditions, we investigate a range of equispaced initial load factors in all examples.

5.1. Two bar truss

We first investigate a numerical example for which an analytical solution exists – see Appendix of Pecknold et al. (1985). The structure consists of a two-bar planar truss with vertical and lateral loads applied, as shown in Fig. 1. The material behavior of the bars is governed by a linear elastic constitutive relation using the Green–Lagrange strain tensor conjugated with the 2nd Piola–Kirchhoff stress tensor. The elastic modulus of the material is given by E, and the cross-sectional area of each bar is A.

The normalized equilibrium equations (Pecknold et al., 1985) are:

$$(1-U)(1-R^2) = \lambda_u \tag{26}$$

$$V(R^2 - K^2) = \lambda_v \tag{27}$$

where $U = u/h$, $V = v/h$, $\lambda_u = P_u/AE\sin^3\alpha$, $\lambda_v = P_v/AE\sin^3\alpha$, $R^2 \equiv (1-U)^2 + V^2$, and $K^2 \equiv 1 - 2\cot^2\alpha$. The internal force vector, tangent stiffness matrix, and external load vector are

$$\mathbf{f} = \begin{Bmatrix} (1-U)(1-R^2) \\ V(R^2 - K^2) \end{Bmatrix} \tag{28}$$

$$\mathbf{K} = \begin{bmatrix} 2(1-U)^2 + R^2 - 1 & -2V(1-U) \\ -2V(1-U) & R^2 - K^2 + 2V^2 \end{bmatrix} \tag{29}$$

$$\mathbf{p} = \begin{bmatrix} \lambda_u & \lambda_v \end{bmatrix}^T, \tag{30}$$

respectively. Two loading cases will be considered: (1) symmetric load case and (2) combined symmetric plus anti-symmetric load

Table 1
Error in the GDCM versus the MGDCM for the symmetric loading case.

$\overline{\Delta\lambda}$	GDCM		MGDCM	
	Steps	Max error %	Steps	Max error %
0.27	15	2.5	15	1.0
0.24	14	3.9	17	0.8
0.21	19	1.7	20	0.6
0.18	20	2.2	23	0.4
0.15	26	0.7	27	0.3
0.12	20	1.7	34	0.2

case. The inclination angle is set at $\alpha = 63.4^\circ$. The problem will be analyzed using the original GDCM and the MGDCM, which has an equivalent constraint as that of the LCALCM. A convergence tolerance of 10^{-10} is used on the incremental displacement vector. The numerical results obtained with each method will be compared to the analytical result.

5.1.1. Symmetric loading case

The external load for the symmetric loading case consists only of the vertical load, such that the external load vector is $\mathbf{p} = [1 \quad 0]^T$. The analytical solution is given by Pecknold et al. (1985)

$$\lambda = U(1-U)(2-U) \tag{31}$$

Two load limits occur at $U = 1 - \sqrt{1/3}$, and $U = 1 + \sqrt{1/3}$ and the corresponding values of the load factor are $\lambda = +2\left(1/3\right)^{3/2}$ and $\lambda = -2\left(1/3\right)^{3/2}$, respectively. For each of the GDCM and the MGDCM, the number of steps and maximum errors are shown in Table 1 for various choices of the initial load factor, $\overline{\Delta\lambda}$. The load factor is kept fixed and the number of steps is adjusted so that the numerical solutions reach $U \geq 2$. The error, which represents the quality of the equilibrium path, is computed at every two sequential steps by calculating the relative error between the analytical solution and the numerical solution. The maximum error is reported in Table 1. The maximum error of the MGDCM for a given $\overline{\Delta\lambda}$ is significantly lower than that of the GDCM.

The plot of U versus λ for the case of $\overline{\Delta\lambda} = 0.24$ is shown in Fig. 2. The behavior of the methods in the rest of the cases shown in Table 1 is similar to this case, so we only show one plot for brevity. The larger error of the GDCM is due mostly to the behavior near limit points, in which the converged solutions skip over portions of the equilibrium path.

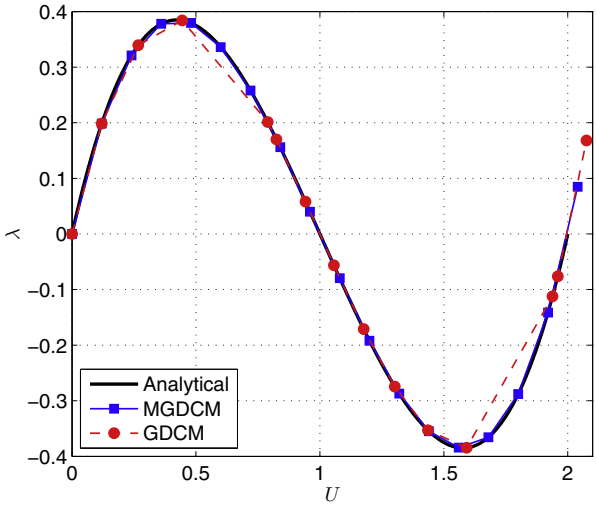

Fig. 2. Equilibrium path, U versus λ, for the symmetric loading case with $\overline{\Delta\lambda} = 0.24$.

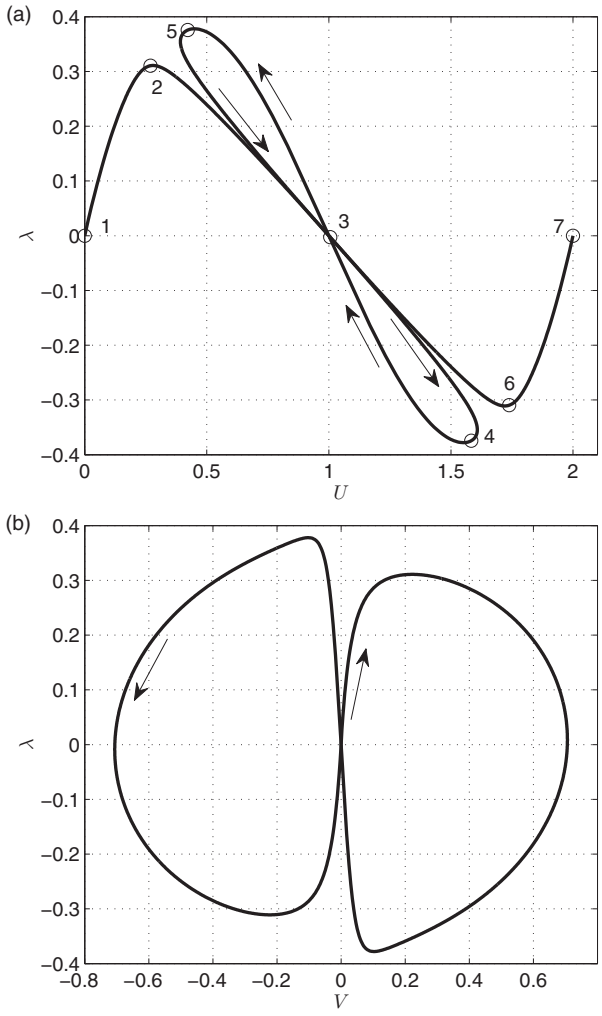

Fig. 3. Analytical solution for the two bar truss subjected to the combined loading case. (a) U versus λ and (b) V versus λ.

5.1.2. Combined proportional loading case

The external load for the combined symmetric plus asymmetric loading case consists of both the vertical and horizontal load. Let $\mathbf{p} = [1 \quad \varepsilon]^T$, where ε is assumed to be 0.05. Again, the reader is directed to the Appendix of Pecknold et al. (1985) for the explicit analytical solution. Four load limits occur at (0.2794, 0.2220), (1.5511, 0.1026), (0.4489, −0.1026), (1.7206, −0.2220) and the corresponding load factors are 0.3109, −0.3779, 0.3779, and −0.3109, respectively. The analytical solution is plotted in Fig. 3, where the arrows indicate the direction of the path. The U versus λ trajectory is broken into segments, which will indicate by the label number shown in Fig. 3(a). For example, the segment between label 1 and label 2 in, will be referred to as segment 1–2. The entire path is given eight segments: 1-2, 2-3, 3-4, 4-3, 3-5, 5-3, 3-6, and 6-7.

The errors between the analytical solution and each of the GDCM and MGDCM are shown in Table 2 for various choices of the load factor, $\overline{\Delta\lambda}$. The error is computed the same way as it was for the symmetric loading case. Of the load factors used in this study, the GDCM only converges when $\overline{\Delta\lambda} = 0.19$, but the error is significantly higher than it is for the MGDCM with the same load factor. In all other cases investigated, the GDCM either does not converge (indicated by "N/C" in Table 2) or the solution jumps to a previously converged portion of the curve during path recovery (indicated by "N/A" in Table 2). Plots of U versus λ and V versus λ are shown in Figs. 4 and 5, respectively, for the values of $\overline{\Delta\lambda}$ shown in Table 2.

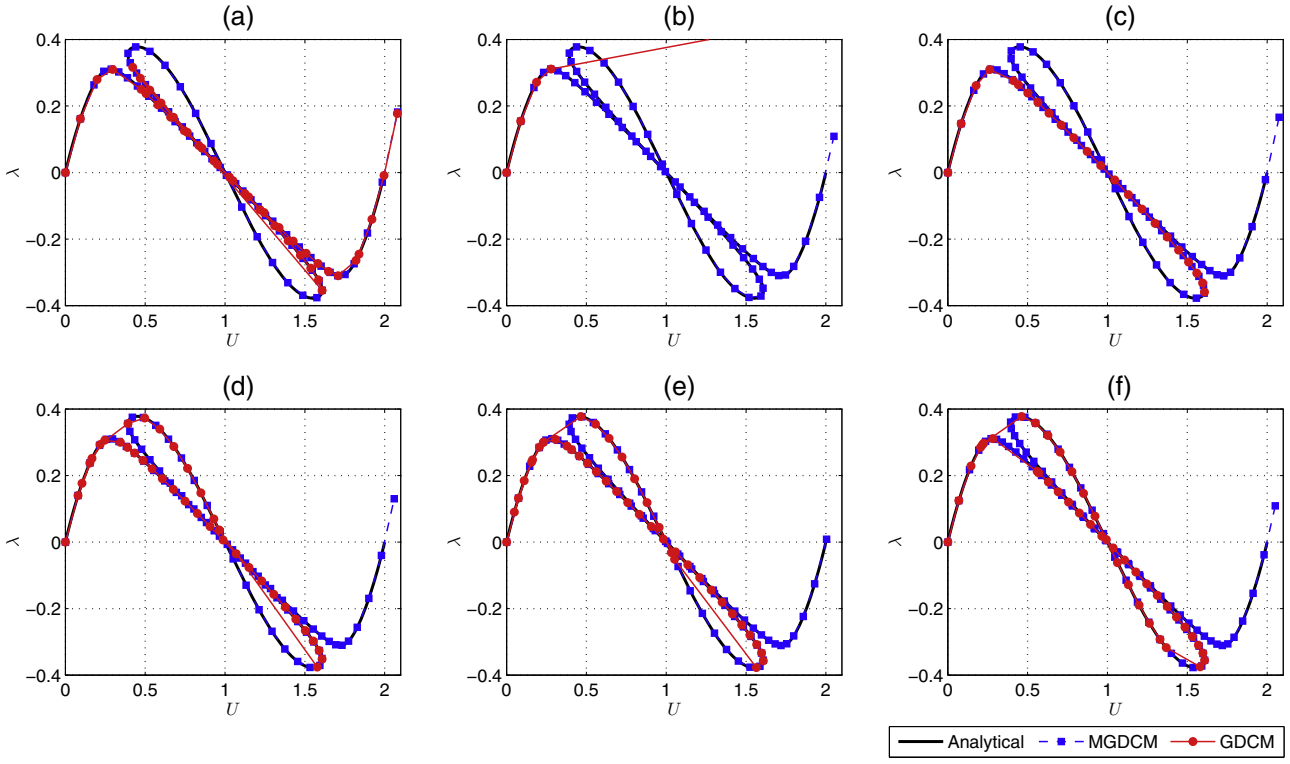

Fig. 4. Equilibrium paths, U versus λ, for the combined loading case (a) $\overline{\Delta\lambda} = 0.19$, (b) $\overline{\Delta\lambda} = 0.18$, (c) $\overline{\Delta\lambda} = 0.17$, (d) $\overline{\Delta\lambda} = 0.16$, (e) $\overline{\Delta\lambda} = 0.15$, and (f) $\overline{\Delta\lambda} = 0.14$.

When $\overline{\Delta\lambda} = 0.19$ the method successfully captures the segments 1-2, 2-3, and 3-4 (cross reference Fig. 3(a)), but skips segments 3-4 and 4-5 and jumps to a portion of curve on segment 5-3, then captures the remainder of the path. When $\overline{\Delta\lambda} = 0.18$ the method only captures the segment 1-2, then skips the entire portion of the curve of interest and converges at a later part of the curve not shown here. The method does not converge at the second load limit point when $\overline{\Delta\lambda} = 0.17$. The behavior when $\overline{\Delta\lambda} = 0.16$, 0.15 and 0.14 is similar: segments 1-2, 2-3, and 3-4 are successfully captured, but all or some of segment 3-4 is skipped. The

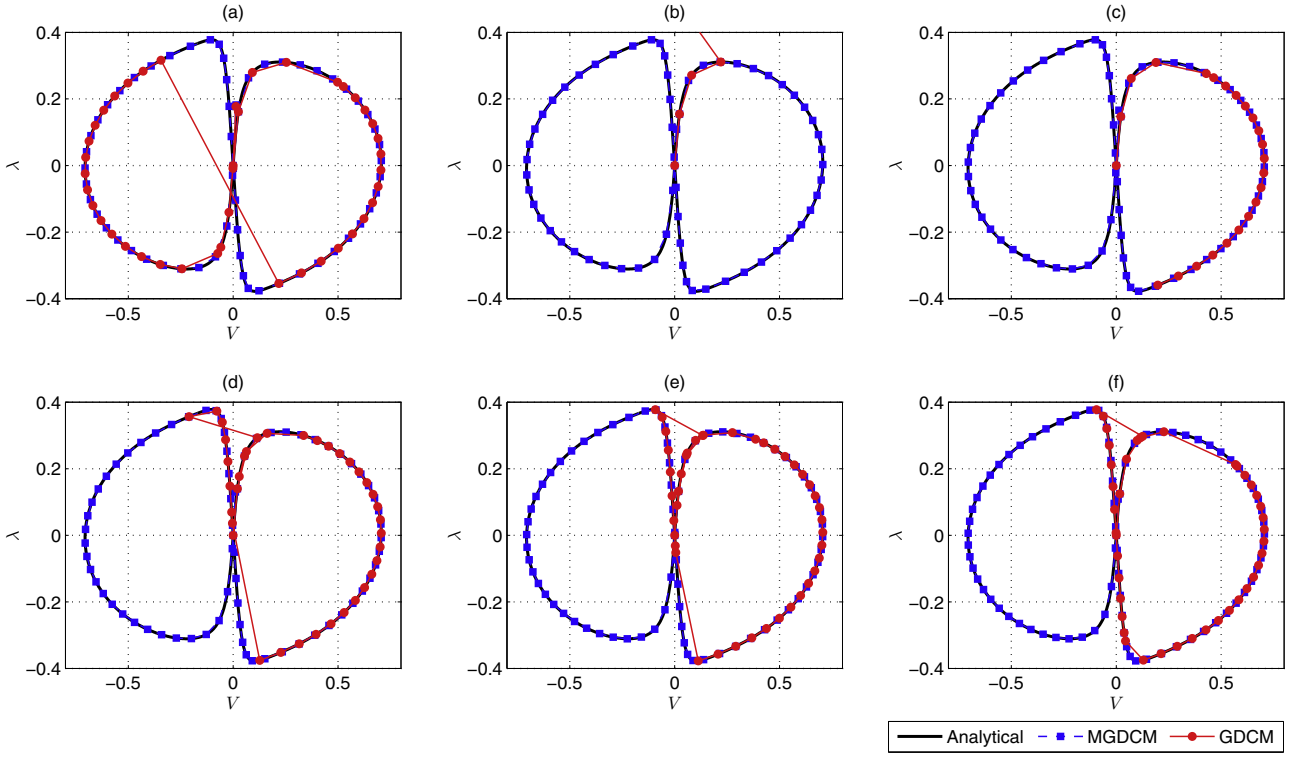

Fig. 5. Equilibrium paths, V versus λ, for the combined loading case (a) $\overline{\Delta\lambda} = 0.19$, (b) $\overline{\Delta\lambda} = 0.18$, (c) $\overline{\Delta\lambda} = 0.17$, (d) $\overline{\Delta\lambda} = 0.16$, (e) $\overline{\Delta\lambda} = 0.15$, and (f) $\overline{\Delta\lambda} = 0.14$.

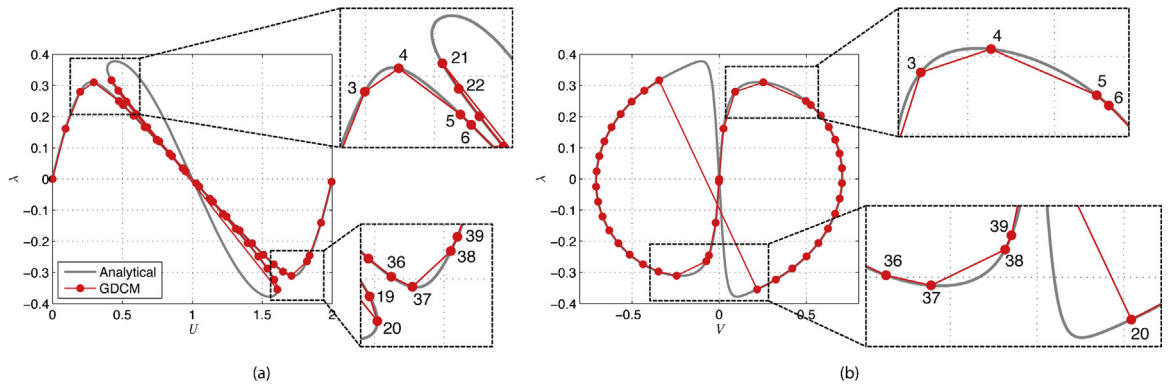

Fig. 6. Equilibrium path with zoomed in areas for $\overline{\Delta\lambda} = 0.19$. (a) U versus λ and (b) V versus λ.

Table 2
Error in the GDCM versus the MGDCM for the combined loading case.

$\overline{\Delta\lambda}$	GDCM		MGDCM	
	Steps	Max error %	Steps	Max error %
0.19	12	18.1	59	2.5
0.18	N/A	N/A	62	2.4
0.17	N/C	N/C	66	2.6
0.16	N/A	N/A	70	2.0
0.15	N/A	N/A	74	1.5
0.14	N/A	N/A	80	1.5

N/A = solution jumps to a previously converged portion of the curve.
N/C = solution not converged.

method correctly traces the segment 3-5, but instead of continuing on to 5-3, the method jumps back to segment 1-2 and traces backwards towards the origin.

We further elaborate on the GDCM for the case where $\overline{\Delta\lambda} = 0.19$ to demonstrate how the load factor increment is overestimated in the vicinity of load limit points. The load versus displacement plots for the GDCM with zoomed in regions are shown in Fig. 6. The plot of U versus V is shown in Fig. 7, in which the analytical solution, GDCM solution, and location of load limit points are indicated. The first load limit point occurs near step 4, and we see rather large jump between steps 4 and 5. The jump is explained by the denominator of the GSP, i.e. $\Delta\mathbf{u}_{p_1}^3 \cdot \Delta\mathbf{u}_{p_1}^4$. The components of these vectors are (1.290551, 1.41579) and (−9.010711, −16.687993), respectively, which results in an inner product (GSP denominator) of 35.254757, and a load factor increment of −0.016314594. If instead, the denominator of the GSP only uses information from the current step to determine the load factor increment, as is the case for the MGDCM, i.e. $\Delta\mathbf{u}_{p_1}^4 \cdot \Delta\mathbf{u}_{p_1}^4$, then the result is 359.6820231, leading to a load factor increment of −0.005107757. Therefore, the GDCM yields a load factor increment that is 219.4% larger than that of the MGDCM. Then, to move to step 6, the GDCM step becomes 57.6% smaller than the MGDCM counterpart. Despite the variability in the size of the load factor, the GDCM is able to capture the first load limit point.

The next load limit points fall between steps 20 and 21, but they are skipped by the GDCM. The denominator of the GSP in the GDCM is 11.46312976, while the MGDCM is 14.29454495. This results in a load factor increment of −0.028611324 for the GDCM and −0.025621491 for the MGDCM. The GDCM load factor increment is only 11.7% larger than that of the MGDCM, but this is large enough to skip the trajectory between steps 20 and 21. This demonstrates that especially in areas of high curvature, the size of the load increment factor should only rely on information from a the current step. Even a slight overestimation can cause the method to skip over important areas of the equilibrium curve.

The behavior at the final load limit point, which occurs near steps 37 and 38, is similar to that at the first load limit point. The GDCM load factor increment is 110.9% greater than the MGDCM between step 37 and 38. Then, to recover and reach step 39, the GDCM step is small, 75.7% smaller than that of the MGDCM.

5.2. Twelve bar truss

The next example is a twelve bar truss structure, shown in Fig. 8, which reduces to a three degree-of-freedom system due to

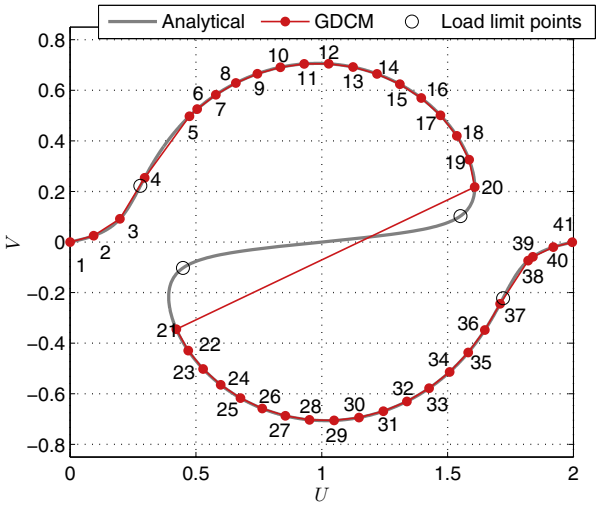

Fig. 7. U versus V for the combined loading case with $\overline{\Delta\lambda} = 0.19$.

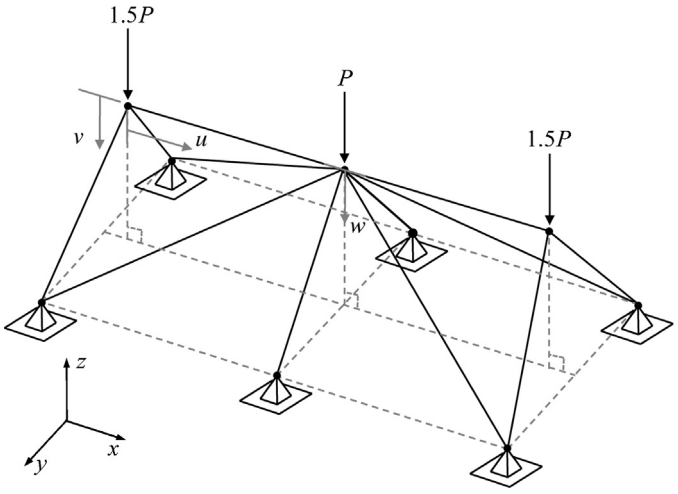

Fig. 8. Schematic of twelve bar truss.

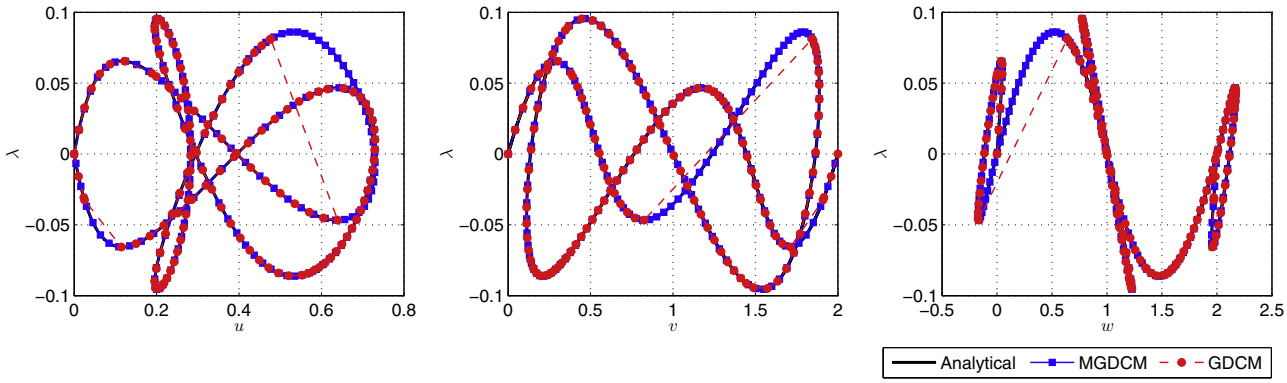

Fig. 9. Equilibrium paths for the twelve bar truss with $\overline{\Delta\lambda} = 0.018$. (a) u versus λ, (b) v versus λ and (c) w versus λ.

Table 3
Error in the GDCM versus the MGDCM for the twelve bar truss.

$\overline{\Delta\lambda}$	GDCM		MGDCM	
	Steps	Max error %	Steps	Max error %
0.022	128	0.6	135	0.3
0.021	130	1.1	141	0.3
0.020	141	0.7	148	0.3
0.019	N/C	N/C	156	0.4
0.018	131	3.5	165	0.3
0.017	169	0.5	175	0.3

N/C = solution not converged.

symmetry. The material behavior of the bars is governed by a linear elastic constitutive relation using the Green–Lagrange strain tensor conjugated with the 2nd Piola–Kirchhoff stress tensor. The elastic modulus of the material is given by E, and the cross-sectional area of each bar is A. The problem has been studied with the GDCM method and other nonlinear solution schemes (Yang and Leu, 1991; Krenk and Hededal, 1995; Leon et al., 2011).

We investigate six different initial load factors, shown in Table 3, all of which are smaller than the load factor reported in Leon et al. (2011). In lieu of an analytical solution, the MGDCM was employed with an initial load factor of 0.00005 (resulting in 59,602 steps) as a reference solution. The error was calculated between this reference solution and each of the GDCM and MGDCM at six initial load factors. The results are shown in Table 3. The GDCM converges in five of the six cases, however the error in each case is larger than that of the MGDCM. The GDCM fails to converge when $\overline{\Delta\lambda} = 0.019$. The source of the error for the case of $\overline{\Delta\lambda} = 0.018$ is evident in Fig. 9.

6. Conclusion

In this study, we have shown that a modification to one parameter of the original GDCM constraint equation results in a more robust nonlinear solution scheme. Instead of using information from the previous increment, as is done in the original GDCM, only information from the current increment is used to define the load factor. Analysis of the MGDCM revealed that its constraint equation is equivalent to that of the LCALCM. Detailed numerical studies on structural systems demonstrate that the GDCM fails to capture the equilibrium path for certain choices of the load factor, while the MGDCM closely matches the analytical solution for all chosen values of the load factor. Although we considered only truss systems here, the formulation also performs well in capturing behavior of systems composed of nonlinear beam elements, which include rotational degrees of freedom. Those examples are not shown here for brevity.

Acknowledgements

Sofie E. Leon gratefully acknowledges the support of the National Science Foundation Graduate Research Fellowship. Glaucio H. Paulino is thankful to the Donald B. and Elizabeth M. Willett endowment at the University of Illinois at Urbana-Champaign.

References

Batoz, J.L., Dhatt, G., 1979. Incremental displacement algorithms for nonlinear problems. International Journal for Numerical Methods in Engineering 14, 1262–1267.
Cardoso, E.L., Fonseca, J.S.O., 2007. The GDC method as an orthogonal arc-length method. Communications in Numerical Methods in Engineering 23, 263–271.
Carrera, E., 1994. A study on arc-length-type methods and their operation failures illustrated by a simple model. Computers and Structures 50, 217–229.
Crisfield, M.A., 1981. A fast incremental/iterative solution procedure that handles snap-through. Computers and Structures 13, 55–62.
Crisfield, M.A., 1983. An arc-length method including line searches and accelerations. International Journal for Numerical Methods in Engineering 19, 1269–1289.
Feng, Y.T., Peric, D., Owen, D.R.J., 1996. A new criterion for determination of initial loading parameter in arc-length methods. Computers and Structures 58, 479–485.
Krenk, S., Hededal, O., 1995. A dual orthogonality procedure for non-linear equations. Computer Methods in Applied Mechanics and Engineering 123, 95–107.
Leon, S.E., Paulino, G.H., Pereira, A., Menezes, I.F.M., Lages, E.N., 2011. A unified library of nonlinear solution schemes. Applied Mechanics Reviews 64, 040803.
Pecknold, D.A., Ghaboussi, J., Healey, T.J., 1985. Snap-through and bifurcation in a simple structure. Journal of Engineering Mechanics 111, 909–922.
Ramm, E., 1980. Strategies for tracing the nonlinear response near limit points. In: Wunderlich, W., Stein, E., Bathe, K.-J. (Eds.), Europe-US Workshop 'Nonlinear Finite Element Analysis in Structural Mechanics', 1981. Springer-Verlag, Berlin, Bochum, Germany, pp. 63–89.
Riks, E., 1972. The application of Newton's method to the problem of elastic stability. Transactions of the ASME: Journal of Applied Mechanics 39, 1060–1066.
Riks, E., 1979. An incremental approach to the solution of snapping and buckling problems. International Journal of Solids and Structures 15, 529–551.
Ritto-Correa, M., Camotim, D., 2008. On the arc-length and other quadratic control methods: established, less known and new implementation procedures. Computers and Structures 86, 1353–1368.
Wempner, G.A., 1971. Discrete approximations related to nonlinear theories of solids. International Journal of Solids and Structures 1, 1581–1599.
Yang, Y.B., Leu, L.J., 1991. Constitutive laws and force recovery procedures in nonlinear analysis of trusses. Computer Methods in Applied Mechanics and Engineering 92, 121–131.
Yang, Y.B., Shieh, M.S., 1990. Solution method for nonlinear problems with multiple critical points. AIAA Journal 28, 2110–2116.